

Harnessing microbially generated power on the seafloor

Leonard M. Tender^{1*}, Clare E. Reimers^{2*}, Hilmar A. Stecher III², Dawn E. Holmes³, Daniel R. Bond³, Daniel A. Lowy⁴, Kanoelani Pilobello⁴, Stephanie J. Fertig⁴, and Derek R. Lovley³

Published online: 1 July 2002, doi:10.1038/nbt716

In many marine environments, a voltage gradient exists across the water–sediment interface resulting from sedimentary microbial activity. Here we show that a fuel cell consisting of an anode embedded in marine sediment and a cathode in overlying seawater can use this voltage gradient to generate electrical power *in situ*. Fuel cells of this design generated sustained power in a boat basin carved into a salt marsh near Tuckerton, New Jersey, and in the Yaquina Bay Estuary near Newport, Oregon. Retrieval and analysis of the Tuckerton fuel cell indicates that power generation results from at least two anode reactions: oxidation of sediment sulfide (a by-product of microbial oxidation of sedimentary organic carbon) and oxidation of sedimentary organic carbon catalyzed by microorganisms colonizing the anode. These results demonstrate in real marine environments a new form of power generation that uses an immense, renewable energy reservoir (sedimentary organic carbon) and has near-immediate application.

An immense energy reserve sits on the seafloor in the form of oxidizable organic carbon resulting primarily from sedimentation of phytoplankton detritus. Vast regions of the seafloor have accumulated sediments meters thick containing 0.1–10% organic carbon by weight¹. The typical energy density of such sediments based on 2.0% organic carbon content² and complete oxidation by oxygen is 6.1×10^4 J/L (17 W h/L)^{3–5}, a remarkable value if sediment volume (6.3×10^{14} liters for the Gulf of Mexico¹, for example) is considered. Microorganisms, limited by the oxidant supply of overlying seawater, use a small portion of this energy reserve, and in doing so create a voltage drop as large as 0.8 V within the top few millimeters to centimeters of sediment surfaces^{6,7}. This voltage gradient results from depletion of oxygen by sediment surface-dwelling microorganisms and metazoans causing microorganisms farther down to use a succession of less potent oxidants (such as sulfate) and generate, as by-products, more potent reductants (such as sulfide) with increasing sediment depth^{3,4}.

Here we report the *in situ* use of benthic voltage gradients to generate sustained electrical power. Two fuel cells were deployed in two coastal marine environments: a boat basin carved into a salt marsh near Tuckerton, New Jersey and the Yaquina Bay Estuary near Newport, Oregon. Each fuel cell consisted of a graphite anode embedded in sediment and a graphite cathode suspended in overlying seawater. The anode and cathode of each fuel cell were connected by an external circuit containing a resistive load capable of dissipating power at either constant voltage or constant current by feedback control of resistance. The natural separation of oxygen-rich seawater (cathodic reactant) and organic carbon-rich sediment (anodic reactant) eliminates the need for a two-compartment cell and a semipermeable membrane for power generation. Placement of the anode into sediment initially disrupts the voltage gradient, which re-establishes itself on the order of days.

Analysis of sediment collected at the Tuckerton site indicated reduced carbon contents of 4–6% (dry weight) arising from marine phytoplankton detritus and the marsh grass *Spartina alterniflora*. Sediment at the Newport site had reduced carbon contents of 2–6% by weight (highest values near the sediment surface) derived primarily from marine phytoplankton and macroalgae, and from the sea grass *Zostera marina*. A second fuel cell through which no current flowed (open circuit) was deployed at each site to serve as a control for post-retrieval sediment and microbial analysis.

Results and discussion

Power generation. Voltage–current and power–current properties of both fuel cells (Fig. 1) indicate the optimal current or voltage ranges at which each fuel cell can be operated to maximize power generation. Current can be sustained in both marine environments, indicating that net oxidation of marine sediment constituents occurs at the anodes and net reduction of seawater constituents occurs at the cathodes. This result is consistent with the use of noncorroding graphite electrodes as anodes in microbial fuel cells⁸ and as cathodes in seawater batteries⁹. Furthermore, the results are consistent with the expected voltage–current and power–current density properties of a fuel cell¹⁰: power seems limited by electrode kinetics at low current density, by mass transfer of charge-compensating ions between electrodes at intermediate current density, and by mass transfer of one of the electrode reactants at high current density.

The Newport deployment (maintained from January 2001 to January 2002) was used in part to assess the long-term ability of a fuel cell to produce current at a constant voltage. From July 17 to November 30, 2001, power density averaged $\sim 28 \text{ mW/m}^2$ at 0.27 V (Fig. 2A), and was steady except for three incidents of power reduction attributed to

¹Center for Bio/Molecular Science and Engineering, Naval Research Laboratory, Code 6900, 4555 Overlook Avenue, SW, Washington, DC 20375. ²Hatfield Marine Science Center, Oregon State University, 2030 SE Marine Science Drive, Newport, OR 97365. ³Department of Microbiology, 106N Morrill IV N, University of Massachusetts, Amherst, MA 01003. ⁴Nova Research, Inc., 1900 Elkin Street, Alexandria, VA 22308.

*Corresponding authors (lmt@cbmse.nrl.navy.mil and clare.reimers@hmsc.orst.edu).

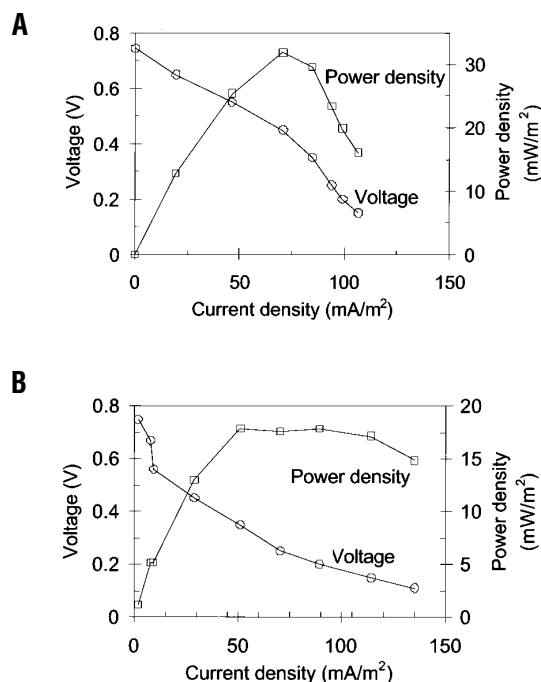


Figure 1. Polarization properties. (A) Voltage and power density vs. current density characterization of fuel cell deployed at Newport site, recorded March 21, 2001. (B) Voltage and power density vs. current density characterization of fuel cell deployed at Tuckerton site, recorded January 22, 2001. Data was obtained by stepwise reduction of cell voltage followed by measurement of current through the external circuit after sufficient time elapsed for current to stabilize (>10 min). Current density (mA/m²) was calculated by normalization of current to the electrode footprint area (0.183 m²); power density (mW/m²) was calculated as the product of voltage and current density.

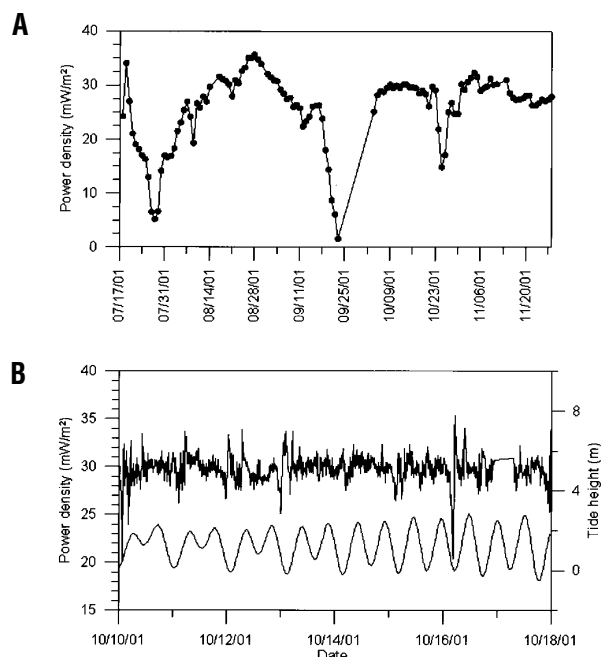


Figure 2. Long-term power density. (A) Daily record of average power density of the active fuel cell deployed at the Newport site. Cell voltage was maintained at 0.27 V. Episodic power reductions are attributed to sedimentation around the cathode. During one such event, cell voltage fell below measurement range of the load resulting in the large gap in late September. On October 2, divers cleared sediment from around and under the cathode resulting in recovery and stabilization of power. Data gaps occurred on six other days due to problems with the recording computer. (B) Eight-day example of tidal time-scale variations in power density recorded every 10 min. Top record, power density. Bottom record, tide height.

episodic coverage of the cathode with sediment and macroalgal detritus as a result of the fuel cell's location in a sheltered cove seasonally inundated by benthic macroalgae. Small to moderate sinusoidal power anomalies observed on a tidal timescale (Fig. 2B) are likely due to combinations of environmental variables associated with estuaries such as temperature, salinity, water velocity, short-term sedimentation events, and sediment bioirrigation.

The Tuckerton deployment (January 2001–August 2001) was used to test power output under varying current and voltage conditions. After 224 days of operation, we retrieved the active (power generating) and control fuel cells from the Tuckerton site and collected core samples of sediment from above and below each anode and scrapings of the graphite anodes. During the first and last weeks of operation, the active fuel cell generated maximum power of 26.6 mW/m² and 25.4 mW/m²,

Table 1. Percentage of 16S rDNA clones recovered from anode surfaces belonging to major phylogenetic groups

Bacterial group	Control (no current)	Active (current)
α -Proteobacteria	17	3
γ -Proteobacteria	21	9
ϵ -Proteobacteria	3	0
δ -Proteobacteria:		
<i>Desulfuromonas</i> spp.	9	45
<i>Desulfobulbus/Desulfocapsa</i> spp.	1	24
Other	13	7
Cytophagales	6	5
<i>Clostridium/Bacillus</i> spp.	5	3
Other	25	4

respectively, indicating remarkable stability in spite of expected electrode fouling. Typical power generation in response to programmed periods of fixed current was constant, whereas voltage rose rapidly upon reduction in current, characteristic of the rechargeable reaction environment around both electrodes (Fig. 3).

Chemical analysis. Comparison of pore-water chemistry near the active and control anodes of the Tuckerton fuel cells yields insights into the mechanisms of power generation. A linear sulfide gradient above and below the active anode and complete sulfide depletion at the anode surface (Fig. 4A) indicate mass transfer–limited oxidation of sediment sulfide at the anode. Application of Fick's first law of diffusion¹¹ using the average sulfide gradient (2.8×10^{-7} mol/cm⁴) and a diffusion coefficient for sulfide through sediment of 1.3×10^{-5} cm²/s at 25°C (the average temperature at the Tuckerton deployment site during August 2001)¹² yields a sulfide flux to the surface of the active anode of 3.6×10^{-4} mol/cm² s. Assuming that two electrons are transferred per sulfur atom in the oxidation of sulfide to elemental sulfur¹³, a current density of 14 mA/m² (based on footprint area of the anode) is expected from the calculated sulfide flux. (Oxidation of sulfide to elemental sulfur is consistent with scanning electron microscopy (SEM) observations of a precipitate on the active anodes and with laboratory studies we have conducted in which electricity was generated from anodes immersed in sterile sulfide-rich media.) Comparison to the measured average current density (35 mA/m²) during the last 23 days of operation (the minimum time required to maintain the observed sulfide depletion zone, t) indicates that other mechanisms contribute to power generation ($t = d^2/4D$ where d is the thickness of the sulfide diffusion layer (10 cm), and D is the diffusion coefficient for sulfide through sediment)¹¹.

Microbial analysis. Analysis of 16S rDNA sequences from microorganisms found in the anode scrapings provides insights into such mechanisms (Table 1). Power generation results in specific enrichment of microorganisms in the delta subclass of the Proteobacteria colonizing the anode of the active fuel cell (76% of the 16S rDNA sequences recovered from the anode of the active fuel cell were in the delta subgroup of Proteobacteria compared with 23% recovered from the anode of the control; Table 1). Furthermore, 59% of the delta Proteobacteria enriched were most closely related to Fe(III) and S⁰-reducing microorganisms in the family Geobacteraceae (>95% similarity to *Desulfuromonas acetoxidans*). This result is similar to results in laboratory studies demonstrating that Geobacteraceae can oxidize acetate, the primary intermediate in the anaerobic degradation of sedimentary organic carbon, and directly transfer electrons to graphite anodes without soluble electron-transfer mediators¹⁴. Laboratory fuel cells using graphite anodes and excess acetate, to which *Desulfuromonas acetoxidans* was added, could sustain current densities of 20 mA/m² (0.13 V) across a 500 Ω load without electron-transfer mediators in solution. Current density increased to 26 mA/m² (0.17 V) when anthraquinone 2,6-disulfonate (AQDS, a compound known to serve as an electron shuttle in the respiration of Geobacteraceae)¹⁵ was added.

Enrichment of dissolved iron near the active anode (Fig. 4B) is consistent with both sulfide depletion (sulfide reacts with soluble Fe(II) to form iron sulfide precipitates) and with the presence of Geobacteraceae. These bacteria are capable of reducing precipitates of Fe(III) to soluble Fe(II). Thus, depletion of sulfide near the active anode would allow Fe(II), generated by Geobacteraceae and other iron-reducing genera, to accumulate in pore water near the active anode relative to the control.

The change in sulfate concentration relative to the change in ammonia (a by-product of microbial oxidation of organic matter) in pore water adjacent to the anode of the active fuel cell is similar to that of pore water adjacent to the anode of the control (Fig. 4C). This suggests that sulfate concentration adjacent to both anodes is primarily determined by depletion of a seawater source by microbial sulfate reduction. Dissimilatory sulfate reduction is commonly described by the following net reaction:

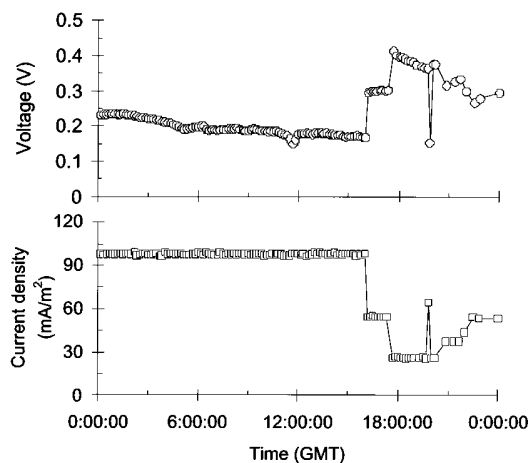
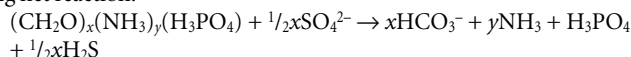


Figure 3. Voltage and current-density record of the active fuel cell deployed at the Tuckerton site recorded August 7, 2001. Data points represent 10-min averages.

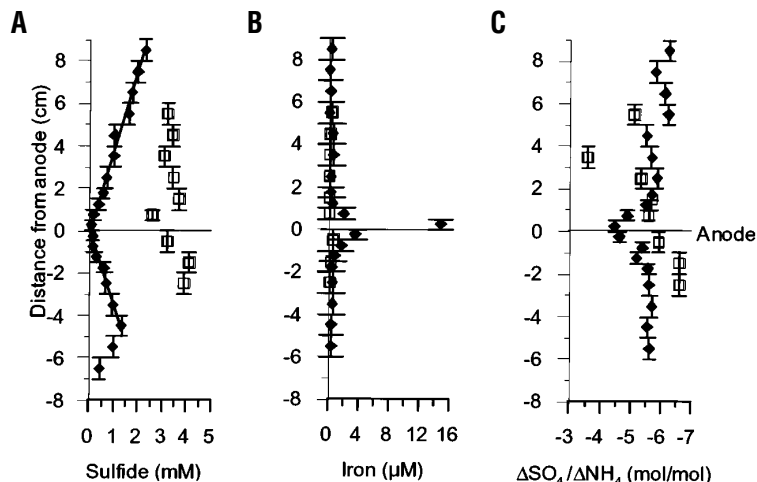


Figure 4. Anode chemical impacts. Comparative pore-water chemistries surrounding the anodes of active (♦) and control (□) cells from the Tuckerton site. Vertical error bars represent the thickness of sediment sections centrifuged to extract pore water.

If this is the only process affecting sulfate and ammonia concentrations, then:

$$\Delta\text{SO}_4^{2-}/\Delta\text{NH}_4^+ = -1/2(x/y) = \text{constant}$$

Nonetheless, modest sulfate enrichment occurs near the active anode (Fig. 4C). This result may reflect microbial oxidation of S⁰ to sulfate with the electrode serving as the electron acceptor, in a manner analogous to previously described microbial oxidation of S⁰ to sulfate with Mn(IV)¹⁶. This is consistent with an observed enrichment of 16S sequences most similar to species in *Desulfobulbus* or *Desulfocapsa* genera (24% of sequences recovered from anodes), as these organisms are known to be capable of sulfur oxidation and disproportionation¹⁷.

Conclusions. The results described here have implications for the development of power supplies that harvest energy from marine environments. Long-term sustained power generation appears limited by reactant flux to the anode (sulfide and organic carbon). This is an environmental factor that promises high power output in certain environments (such as at sulfide-rich vents or near or atop methane hydrate deposits^{18,19}). Furthermore, long-term steady-state power generation is not limited by fouling, which often dramatically changes the surface properties of objects placed in marine environments. Microbial colonization is an important component of fouling. Further investigation of the influence of oxidative current on the anode-colonizing microorganisms may lead to better strategies toward antifouling surfaces. Many marine oceanographic instruments such as integrated conductivity, temperature, and depth sensors, hydrophones, and underwater inductive modems have power requirements on the order of 0.1–1 W with deployment times limited by battery life. A fuel cell that uses abundant fuel and oxidant as they are naturally found has now been shown to operate without fouling for many months in two marine environments. In the one case analyzed, observed microbial enrichment and sulfide depletion suggest that both microbial metabolism with coupled direct electron transfer to the anode and oxidation of sediment sulfide contributed to the observed current. In this specific environment, ~40% of the observed current density (14 mA/m² of 35 mA/m²) could be attributed to oxidation of sediment sulfide. The balance of observed current density (21 mA/m²) is consistent with that sustained in laboratory studies (20–100 mA/m²) by catalytic oxidation of sedimentary acetate by microorganisms colonizing the anode. Most certainly, the relative and absolute contributions of each

mechanism with respect to overall power generation will depend strongly on the specific environment. Other anode reactions, possibly involving microbial consortia and various oxidation states of sulfur, cannot be ruled out and need further investigation. By scaling up the approach described here, long-term (indefinite) power may be supplied by such fuel cells to marine instruments in the near future.

Experimental protocol

Fuel cells. Electrodes consisted of graphite discs (LG graphite grade 10, Graphite Engineering & Sales, Greenville, MI) of 48.3 cm diameter and 1.3 cm thickness drilled with a pattern of 790 evenly spaced holes of 0.64 cm diameter. Electrodes were used as received or lightly sanded. Electrical connection to the anode and cathode of each active fuel cell was made in the following manner. A water-insulated, pluggable, single-conductor, oceanographic, electrical bulkhead connector (Impulse Enterprise, San Diego, CA) was joined to each electrode by silver epoxy (Epoxy Technology, Billerica, MA) encapsulated with water-insulating epoxy (Dexter Corporation, Seabrook, NH). Matching single-conductor oceanographic cables attached to these connectors electrically connected the anode and cathode of each active fuel cell to pluggable bulkhead connectors wired to a computer-controlled resistive load (870, Scribner Associates, Southern Pine, NC) contained within a custom-built oceanographic instrument enclosure. Connections to land-based power (for operation of the load) and computer were provided by additional cables to the enclosure.

The connector–silver epoxy–graphite union of the active cathode at the Newport site failed after 4.5 months (January–May 2001). A new active fuel cell was subsequently deployed at the Newport site (June 2001–January 2002) with electrodes attached directly to the single-conductor oceanographic cables by wrapping a stripped-end section of each copper-conducting wire around a #6 stainless steel screw with 32 threads per inch (6–32) threaded into a hole tapped into each electrode. Each of these cable–graphite unions was then encapsulated into a block of water-resistant epoxy (West System, Gougeon Brothers, Bay City, MI). Polyvinyl chloride (PVC) frames were used for both Newport fuel cells to position each anode ~15 cm below and parallel to the sediment surface and each cathode ~15 cm above and parallel to the sediment surface in overlying seawater. These fuel cells were deployed by divers in water with a mean midtide depth of ~4 m.

Electrodes of both Tuckerton fuel cells were enclosed within 167-liter cylindrical PVC containers (Rubbermaid, Cleveland, OH). Each container had 80 holes of 5.1 cm diameter lined with fiberglass screen. These holes ensured sufficient mass transfer of seawater to the cathode while enabling recovery of sediment above and below the anode with intact geochemical stratification when each fuel cell was retrieved. Before deployment, each container was partially filled with ~50 liters of sediment, the anode was positioned ~10 cm below and parallel to the sediment surface, and the cathode was positioned ~20 cm above and parallel to the sediment surface. The Tuckerton fuel cells were deployed by lowering the containers until they settled into sediment in water with a midtide mean depth of ~1.5 m. These fuel cells settled such that the inner and outer sediment heights were near equal. An integrated conductivity, temperature, and depth meter and an acoustic Doppler current meter were deployed at each site to correlate changing fuel-cell voltage and current with changing environmental properties.

DNA extraction and cloning of 16S rDNA. Electrode surfaces were washed free of sediment with sterile artificial seawater, and scraped vigorously with a sterile razor blade into 1.5 ml TE buffer (10 mM Tris-HCl, 1 mM EDTA, pH 8; Sigma, St. Louis, MO). The miniprep of bacterial genomic DNA protocol²⁰ was used for DNA extraction from the recovered graphite slurry with the following modifications. The pellet was resuspended in TE/sucrose buffer (50 mM Tris-HCl, 10 mM EDTA, pH 8, 6.7% sucrose), SDS (0.5%, final concentration) and lysozyme (1 mg/ml final concentration; Sigma) were added to the suspension, and tubes were incubated at 37°C for 30 min with vortexing every 5 min. After proteinase K treatment (0.1 mg/ml; Sigma) at 37°C for 1 h, MULTIMIX 2 Tissue Matrix (Bio101 Systems, Carlsbad, CA) was added to the suspension. Tubes were then placed in a Mini-BeadBeater (BioSpecs Products, Bartlesville, OK) for 30 s at 550 rpm, DNA was extracted once with chloroform/isoamyl alcohol (24:1; Sigma), and once with phenol/chloroform/isoamyl alcohol (25:24:1;

Sigma). This extracted DNA was further purified with the Wizard DNA Clean-Up System (Promega, Madison, WI). Extractions typically yielded 20–100 µg DNA per 10 cm² of electrode.

In two separate reactions, 16S rDNA was amplified using primers 27F²¹ or 63F²² with 519R²³. The total volume of each PCR mixture was 100 µl, and contained ~60 µg DNA template, 10 µl Qiagen 10× buffer (15 mM MgCl₂), 5 µl buffer Q (Qiagen, Valencia, CA), 8 µl 0.25 µM dNTP solution (Sigma), 60 pmol each forward and reverse primers, 5 µl dimethyl sulfoxide (Sigma), and 3 units Taq polymerase (Qiagen). To ensure sterility, the PCR mixtures were exposed to UV radiation for 10 min before the addition of template and Taq polymerase. PCR amplification was carried out in a DNA Engine thermal cycler (MJ Research, Waltham, MA) with an initial denaturation step of 94°C for 4 min, followed by 35 cycles of 94°C for 30 s, 50°C for 30 s, and 72°C for 45 s with a final extension of 72°C for 7 min. The PCR products from all reactions were pooled and cloned into *Escherichia coli* using the TOPO TA cloning kit, version K2 (Invitrogen, Carlsbad, CA).

Clones were randomly selected from each clone library, and cloned 16S rDNA was amplified from the TOPO vector using M13 forward and M13 reverse primers (Invitrogen). These amplified inserts were incubated for 16 h at 37°C with *Hha*I and *Msp*I (both 4 bp cutters; New England Biolabs, Beverly, MA). The results from the restriction digests were visualized on a 3% (wt/vol) Metaphor agarose gel (BioWhittaker Molecular Applications, Rockland, ME), and clones yielding similar restriction-digest banding patterns were assumed to carry similar 16S rDNA inserts. Plasmids were isolated from cultures showing different banding patterns with the QIAprep Spin Miniprep Kit (Qiagen), and plasmid inserts were sequenced. Sequences were compared to GenBank and Ribosomal Database Project databases using the BLAST²⁴ and SIMILARITY²⁵ algorithms. At least 60 sequences were analyzed for each clone library, and representative sequences were submitted to GenBank (accession nos AY123202–AY123222).

Sediment pore water analysis. Pore waters were extracted by centrifugation from sections of cores of 8 cm diameter and then filtered (0.45 µm). All sample handling was done in a glove bag at 25°C ± 3°C (equal to the average daily *in situ* temperature at Tuckerton Site in August 2001) under a N₂ atmosphere. Samples for quantifying dissolved sulfide concentrations were fixed immediately according to Cline²⁶ and measured spectrophotometrically (Gilford Stasar II, 1 cm path length). Total iron was measured after appropriate sample dilution of acidified samples by flow-injection analysis and spectrophotometric detection following Measures *et al.*²⁷. The detection of iron is achieved through its catalytic effect on the oxidation of N,N-dimethyl-*p*-phenylenediamine dihydrochloride by hydrogen peroxide, producing colored semi-quinone derivatives. Sulfate and chloride concentrations were measured after dilution of nonacidified samples using a DX-500 Ion Chromatograph with AG14 columns (Dionex, Sunnydale, CA). Ammonium was determined using a nutrient autoanalyzer (Alpkem, Clackamas, OR) after a 1:26 dilution:

$$\Delta\text{NH}_4 = -(\text{NH}_4)_{\text{measured}}$$

Pore water sulfate depletion was calculated as

$$\Delta\text{SO}_4 = \left[\left(\frac{\text{SO}_4}{\text{Cl}} \right)_{\text{seawater}} \times [\text{Cl}]_{\text{measured}} \right] - [\text{SO}_4]_{\text{measured}}$$

assuming pore water is buried with the conservative ratio of sulfate to chloride characteristic of seawater.

Acknowledgments

This work was supported by grants from the Office of Naval Research (ONR), the Naval Research Laboratory (NRL), and the Defense Advanced Research Projects Administration (DARPA). We are grateful to Rose Petrecca, Joe Debarro, and staff of the Tuckerton, New Jersey Field Station of Rutgers University, Institute of Marine and Coastal Sciences for assistance in fuel-cell deployment and retrieval. We also thank M. Sommer, R. Emmett, T. Bridgeman, T. Builder, W. Hanshumacher, D. Jacobson, and M. Spencer for diving assistance at the Newport site and L. Annable for field assistance.

Competing interests statement

The authors declare that they have no competing financial interests.

Received 24 January 2002; accepted 7 May 2002

1. Yen, T.F. Chemical aspects of marine sediments. in *Chemistry of Marine Sediments* (ed. Yen, T.F.) 1–38 (Ann Arbor Science Publishers, Ann Arbor, MI, 1977).
2. Cai, W.-J. & Reimers, C.E. Benthic oxygen flux, bottom water oxygen concentration and core top organic carbon content in the deep northeast Pacific Ocean. *Deep-Sea Res. I* **42**, 1681–1699 (1995).
3. Froelich, P.N. *et al.* Early oxidation of organic-matter in pelagic sediments of the eastern equatorial Atlantic–suboxic diagenesis. *Geochim. Cosmochim. Acta* **43**, 1075–1090 (1979).
4. Berner R.A. *Early Diagenesis: A Theoretical Approach* (Princeton Univ. Press, Princeton, NJ, 1980), p. 241.
5. Morel, F.M.M. & Hering, J.G. *Principles and Applications of Aquatic Chemistry* (Wiley, New York, 1993), p. 588.
6. Schindler, J.E. & Honick, K.R. Oxidation-reduction determinations at mud-water interface. *Limnol. Oceanogr.* **16**, 837–840 (1971).
7. Reimers, C.E., Tender, L.M., Fertig, S.J. & Wang, W. Harvesting energy from the marine sediment-water interface. *Environ. Sci. & Technol.* **35**, 192–195 (2001).
8. Palmore, G.T.T. & Whitesides, G.M. Enzymatic conversion of biomass for fuels production. *ACS Sym. Ser.* **566**, 271–290 (1994).
9. Wilcock, W.S.D. & Kauffman, P.C. Development of a seawater battery for deep-water applications. *J. Power Sources* **66**, 71–75 (1997).
10. Hart, A.B. & Womack, J.G. *Fuel Cells. Theory and Application* (Chapman and Hall, London, 1967), p. 54.
11. Bard, A.J. & Faulkner, L.R. *Electrochemical Methods: Fundamentals and Applications* (Wiley, New York, 1980), p. 130.
12. Boudreau, B.P. *Diagenetic Models and their Implementation. Modelling Transport and Reactions in Aquatic Sediments* (Springer, New York, 1997), p. 414.
13. Zhang, L.Z., Lever, A.B.P. & Pietro, W.J. Surface copper immobilization by chelation of alizarin complexone and electrodeposition on graphite electrodes, and related hydrogen-sulfide electrochemistry; matrix-isolation of atomic copper and molecular copper sulfides on a graphite electrode. *J. Electroanal. Chem.* **385**, 191–200 (1995).
14. Bond, D.R., Holmes, D.E., Tender, L.M. & Lovley, D.R. Electrode-reducing microorganisms that harvest energy from marine sediments. *Science* **295**, 483–485 (2002).
15. Lovley, D.R. *et al.* Humic substances as electron acceptors for microbial respiration. *Nature* **382**, 445–448 (1996).
16. Lovley, D.R. & Phillips, E.J.P. Novel processes for anaerobic sulfate production from elemental sulfur by sulfate-reducing bacteria. *Appl. Environ. Microbiol.* **60**, 2394–2399 (1994).
17. Finster, K., Liesack, W. & Thamdrup, B. Elemental sulfur and thiosulfate disproportionation by *Desulfocapsa sulfoexigens* sp. nov., a new anaerobic bacterium isolated from marine surface sediment. *Appl. Environ. Microbiol.* **64**, 119–125 (1998).
18. Sahling, H., Rickert, D., Linke, P., Suess, E. & Lee, R.W. Macrofaunal community structure and sulfide flux at gas hydrate deposits from the Cascadia convergent margin, NE Pacific. *Mar. Ecol. Prog. Ser.* **231**, 121–138 (2002).
19. Kennett, J.P., Cannariato, K.G., Hendy, I.L. & Behl, R.J. Carbon isotopic evidence for methane hydrate instability during quaternary interstadials. *Science* **288**, 128–133 (2000).
20. Ausubel, F.M. *et al.* *Protocols in Molecular Biology* (ed. Chanda, V.B.) (Wiley, New York, 1997).
21. Lane, D.L. in *Nucleic Acid Techniques in Bacterial Systematics* (eds Stackebrandt, E. & Goodfellow, M.) 115–175 (Wiley, Chichester, United Kingdom, 1991).
22. Marchesi, J.R. *et al.* Design and evaluation of useful bacterium-specific PCR primers that amplify genes coding for bacterial 16S rRNA. *Appl. Environ. Microbiol.* **64**, 795–799 (1998).
23. Lane, D.L. *et al.* Rapid-determination of 16S ribosomal-RNA sequences for phylogenetic analyses. *Proc. Natl. Acad. Sci. USA* **82**, 6955–6959 (1985).
24. Altschul, S.F. *et al.* Basic local alignment search tool. *J. Mol. Biol.* **215**, 403–410 (1990).
25. Maidak, B.L. *et al.* A new version of the RDP (Ribosomal Database Project). *Nucleic Acids Res.* **27**, 171–173 (1999).
26. Cline, J.D. Spectrophotometric determination of hydrogen sulfide in natural waters. *Limnol. Oceanogr.* **14**, 454–458 (1969).
27. Measures, C.I., Yuan, J. & Resing, J.A. Determination of iron in seawater by flow injection-analysis using in-line preconcentration and spectrophotometric detection. *Mar. Chem.* **50**, 3–12 (1995).